POLITECNICO DI TORINO
Repository ISTITUZIONALE

Mathematical Characterisation of a Heat-Pipe by means of the Non-Isothermal Cahn-Hilliard Model

(Article begins on next page)

11 April 2024

Mathematical Characterisation of a Heat Pipe by means of the Non-Isothermal Cahn-Hilliard Model

Melania Carfagna, Filomena Iorizzo, Alfio Grillo

Abstract The aim of this contribution is to provide a thorough description of a heat pipe. This is a particular type of heat exchanger used in a variety of industrial applications, such as the cooling of electrical devices and solar cells, the temperature equalisation in spacecrafts, or the reduction of local heat gains in reactors and air-conditioning systems. Usually, lumped parameter models are used to study the behaviour of heat pipes and the thermal ranges in which they work optimally. In the following analysis, a quite comprehensive thermo-fluid dynamic model of the liquid/vapour pair operating in a heat pipe is developed. The model, which accounts for several phenomena taking place in this kind of devices, has the purpose of predicting the optimal thermal range of a given heat pipe, and preventing the occurrence of off-design conditions. The present investigation is done by considering a heat pipe working in zero-gravity conditions, to be used for Aerospace applications.

1 Problem statement - Mathematical and Numerical Issues

A heat pipe is a thermal device used to transport and drain heat from a hot zone to a cold one. It can be differently structured. The one considered here is a metallic tube, filled with a small amount of fluid, and then welded at the ends. One of its two ends is placed in contact with a heat source, while the other one is refrigerated. The thermodynamic conditions of the fluid inside the pipe are such that the liquid and

———————————————

Melania Carfagna
DISMA "G.L.Lagrange", C.so Duca degli Abruzzi 24, 10129, Torino, Italy, e-mail: melania.carfagna@polito.it

Filomena Iorizzo
Argotec s.r.l., via Cervino 52, 10155, Torino, Italy, e-mail: filomena.iorizzo@argotec.it

Alfio Grillo
DISMA "G.L.Lagrange", C.so Duca degli Abruzzi 24, 10129, Torino, Italy, e-mail: alfio.grillo@polito.it

vapour phases of the fluid coexist. The liquid phase evaporates in the hot zone of the tube, while the vapour condenses in the cold one. The processes of evaporation and condensation form a cycle, which takes place at saturation temperature. Usually, this temperature is lower than the one at the atmospheric pressure. More precisely, the thermodynamic cycle experienced by the fluid in the heat pipe consists of the following stages:

- Evaporation of the liquid at the hot end;
- Flux of the produced vapour from the evaporator to the condenser by means of a pressure gradient induced by the thermal difference between the hot and the cold end of the pipe;
- Condensation of vapour at the cold end;
- Reflux of the condensed liquid at the evaporator zone due to a capillary structure that covers the internal wall of the tube.

When the heat pipe works in nominal conditions, the latent heat H_{lv}, which is supplied during evaporation and subtracted during condensation, balances the heat sources and sinks applied from the outside. In principle, this thermal balance maintains the whole heat pipe at almost the same temperature. Nevertheless, in order to control and predict the occurrence of off-design conditions, a non-isothermal model of the heat pipe is required [2].

The Cahn-Hilliard model is widely used to model phenomena such as capillary waves and moving contact lines [1] between two fluids as well as near-critical point phenomena, such as the spinodal decomposition and phase transitions. It describes the interface between two fluid phases as a thin transition layer in which the two phases coexist and form, thus, a mixture. To model the coupling that occurs at the interface between these two weakly miscible [7] (and often weakly compressible) fluids in contact one with each other, it is postulated that the system possesses a Helmholtz free energy density of the type

$$F(\varphi, \nabla \varphi) = \tfrac{1}{2}\lambda |\nabla \varphi|^2 + U(\varphi), \quad U(\varphi) = \tfrac{1}{4}\lambda \varepsilon^{-2}(1-\varphi^2)^2. \tag{1}$$

Here, the term $\tfrac{1}{2}\lambda |\nabla \varphi|^2$ describes a weak interaction between the two phases (this interaction is often referred to as "non-local" in the literature), whereas $U(\varphi)$ is a globally non-convex, double-well potential vanishing at $\varphi = \pm 1$. The field φ is sometimes referred to as "colour function". In this work, it is defined as an affine function of the mass fraction c of one of the two phases, i.e. $\varphi = 2c - 1$. The parameters λ and ε are quantities related, respectively, to the chemical potential of the system at the interface, i.e., the surface tension force σ_{t}, and the thickness of the layer.

The thermodynamic consistency is fulfilled by constitutive relations that ensure the non-negativeness of the entropy production of the system. In particular, this requirement yields a characterisation of the total stress tensor $\boldsymbol{\sigma}$, entropy flux $\boldsymbol{q}_{\text{s}}$, and diffusive mass flux vector $\boldsymbol{J}_{\text{d}}$:

$$\boldsymbol{\sigma} = \boldsymbol{\tau} - p\boldsymbol{I} - \boldsymbol{K}, \tag{2}$$

$$T\boldsymbol{q}_{\mathrm{s}} = \boldsymbol{q} - \dot{\varphi}\left[\nabla.\left(\frac{\partial F}{\partial \nabla \varphi}\right)\right], \tag{3}$$

$$\boldsymbol{J}_{\mathrm{d}} = -\rho \mu \nabla \theta. \tag{4}$$

In (2)–(4), $\boldsymbol{\tau}$ represents the viscous part of the overall stress $\boldsymbol{\sigma}$, p is pressure, $\boldsymbol{K}$ is known as Korteweg stress tensor, $\boldsymbol{q}$ is the heat flux vector, μ is the motility of the liquid/vapour pair, ρ is the mass density of the mixture, and θ is the chemical potential, which reads

$$\rho \theta = 2\frac{\lambda}{\varepsilon^2}\left(-\varepsilon^2 \Delta \varphi + (\varphi^2 - 1)\varphi\right) - 2\frac{\partial \rho}{\partial \varphi}\frac{1}{\rho}(p + F). \tag{5}$$

The superimposed dot denotes the substantial derivative, i.e. $\dot{\varphi} = \partial_t \varphi + \nabla \varphi . \boldsymbol{u}$, with $\boldsymbol{u}$ being the velocity of the two-fluid system. For a quasi-immiscible pair, as the one considered in this discussion, the Korteweg stress tensor $\boldsymbol{K}$ is usually related to the surface tension force [5].

By substituting (5) into (4), and considering the balance laws of mass, linear momentum and energy, the following system of partial differential equations is obtained

$$\nabla \cdot \boldsymbol{u} = \frac{\rho_{\mathrm{l}} - \rho_{\mathrm{v}}}{\rho_{\mathrm{l}}\rho_{\mathrm{v}}}\rho\left(\nabla \cdot \left[-2\mu\nabla\left(\frac{\lambda}{\varepsilon^2}\psi\right)\right] + \frac{\Gamma_{\mathrm{v}}}{\rho}\right), \tag{6}$$

$$\dot{\varphi} = -2\nabla \cdot \left[-2\mu\nabla\left(\frac{\lambda}{\varepsilon^2}\psi\right)\right] - 2\frac{\Gamma_{\mathrm{v}}}{\rho}, \tag{7}$$

$$\psi = -\varepsilon^2 \Delta \varphi + (\varphi^2 - 1)\varphi, \tag{8}$$

$$\rho\dot{\boldsymbol{u}} = \nabla \cdot (\boldsymbol{\tau} - p\mathbf{I}) - \boldsymbol{F}_{\mathrm{st}}, \tag{9}$$

$$\rho C_{\mathrm{p}}\dot{T} = \nabla \cdot (k\nabla T) + \boldsymbol{\tau} : \boldsymbol{d} + \dot{\varphi}\lambda\Delta\varphi + H_{\mathrm{lv}}\Gamma_{\mathrm{v}}. \tag{10}$$

Here, ρ_{l} and ρ_{v} denote, respectively, the mass densities of the liquid and vapour, Γ_{v} is the evaporation/condensation mass flow rate, which has been modeled by means of the *Knudsen* relation for the liquid/vapour phase change:

$$\Gamma_{\mathrm{v}} = C\sqrt{\frac{M}{2\pi R}}\left(\frac{p_{\mathrm{sat}}(T_{\mathrm{l}})}{\sqrt{T_{\mathrm{l}}}} - \frac{p_{\mathrm{v}}}{\sqrt{T_{\mathrm{v}}}}\right), \tag{11}$$

with M being the molar mass of the liquid and R the Universal Gas Constant. The subscripts "l" and "v" indicate, respectively, whether a given physical quantity is evaluated in the liquid or in the vapour phase. The term C is an accommodation coefficient to be adapted to the considered fluid [3, 6]. The saturation pressure p_{sat} appearing in Eq. (11), also known as vapour tension of the substance, is evaluated punctually in the interior of the heat pipe by means of the *Clausius-Clapeyron* formula [6]

$$p_{\mathrm{sat}}(T) = p_0 \exp\left[\frac{MH_{\mathrm{lv}}}{R}\left(\frac{1}{T} - \frac{1}{T_0}\right)\right]. \tag{12}$$

The term $\boldsymbol{F}_{\mathrm{st}} = \nabla.\boldsymbol{K}$, under appropriate assumptions, can be written as

$$\boldsymbol{F}_{\mathrm{st}} = -\frac{\lambda}{\varepsilon^2} \psi \nabla \varphi.$$

The parameters, which refer to the two-fluid system as a mixture, i.e., the specific heat at constant pressure C_{p}, the thermal conductivity k, $\boldsymbol{u}$ and ρ, are defined as usually done for a two-constituent mixture in the framework of Mixture Theory. The term $\boldsymbol{d} = \mathrm{sym}(\nabla \boldsymbol{u})$ is the symmetric part of the velocity gradient.

Equations (6)–(10) are considered hereafter to model the two-fluid system in the heat exchanger. Equation (6) represents the mass balance law of the liquid/vapour system as a whole. It states that the velocity flux of the system's centre of mass is not solenoidal. This differs from many other models (cf., e.g., [4, 8]), which rely on the constraint that the velocity field is divergence-free. Equation (7) represents the modified concentration balance law of one of the two phases. Equation (8) is an auxiliary equation, introduced to eliminate the fourth order derivative of the colour function φ, which would otherwise arise in the first term on the right-hand-side of Eq. (7). Finally, Eqs. (9) and (10) are, respectively, the local forms of the balance laws of linear momentum and energy of the system as a whole.
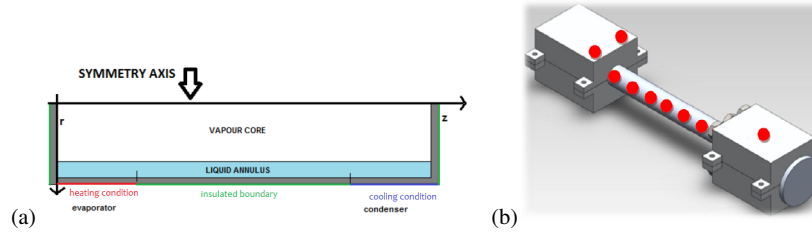
Fig. 1 (a) Axially symmetric geometry of the system considered in the numerical simulations. (b) The experimental apparatus. The red dots correspond to the positions of the thermocouples.

The weak form of (6)–(10) has been implemented in a commercial Finite Element Software, by modifying an already existing model, in which the non-standard terms, i.e., the ones linked to the presence of a thermal field, the phase change and the weak miscibility, are not included. For numerical purposes, in (6)–(10) the contributions of compressibility have been neglected. The parameters ε, λ and μ in Eq. (1) are defined as in [8]. The parameters $\rho_{\mathrm{l}}, \rho_{\mathrm{v}}, H_{\mathrm{lv}}, \sigma_{\mathrm{t}}, C_{\mathrm{p}}, k$, which define the nature of the chosen working fluid, are here defined as polynomial functions of the temperature. We underline that, depending on which requirements the heat exchanger has to satisfy, any working fluid can be chosen (e.g., liquid metals, water, ammonia, acetone, alcohol, nitrogen and helium) and, in principle, it can be characterized by the same set of parameters. In this contribution, the chosen working fluid is covered by a non-disclosure agreement.

Finally, the geometric setting employed in the performed numerical simulations is schematically shown in Fig. 1-a.

2 Validation and Results

The numerical model was validated by experimental data provided by Argotec s.r.l. that designed the heat pipe and the experimental apparatus and performed the test campaign. The pipe was heated at one of its two ends (where an imposed heat flux is prescribed) by means of resistors, and cooled down at the other end, which was inserted in a cooling jacket. The latter one was connected with a thermal bath via a bundle of tubes in which a refrigerating fluid was conveyed. The remaining part of the pipe was thermally insulated and, thus, referred to as "adiabatic zone".

The output data were obtained by positioning thermocouples (with a precision of 1 K) along the pipe, as shown in Fig. 1-b. The temperature at each thermocouple position was measured at different instants of time until the system reached stationary working conditions. The system described above, and the experiments conduced on it, were simulated for different values of the thermal power supplied to the evaporation zone. The results obtained by the model presented in this contribution were validated by comparison with the experimental outputs referred to the system's stationary working conditions. The experimental and simulated outcomes are reported in Fig. 2, and refer to the values of temperature on the outer wall of the heat pipe, evaluated with respect to a reference temperature.

Fig. 2 Validation of the model: Numerical and experimental thermal outputs on the outer wall of the pipe. Diamonds and triangles correspond to the positions of the thermocouples.
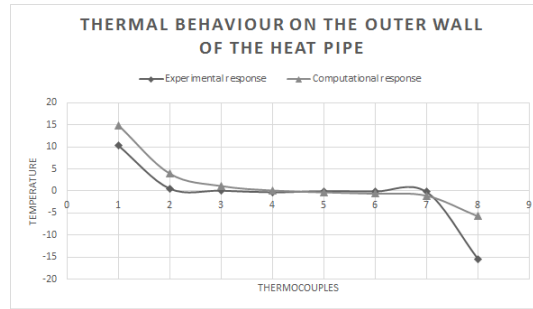
In the adiabatic zone, the relative percentage of error between the measured temperature and the simulated one is below 1% for all the performed simulations.

After validating the model, it has to be assessed whether or not the heat pipe works in nominal conditions. This investigation is carried out by analyzing the temperature, pressure and velocity fields as well as the chemical potential in different zones of the pipe.

The first result presented here (see Fig. 3-a) refers to the evaluation of the discrepancies between the saturation state (p_{sat}, T_{sat}) and the output state of the system (p, T). Hereafter, we refer to T_l and p_l as the output values taken at the bottom of the liquid film, and T_v and p_v as the values taken on the symmetry axis of our numerical representation of the heat pipe. If the pair (p_v, T_v), especially in those points corresponding to the adiabatic zone, exhibits strong deviations from the saturation state (p_{sat}, T_{sat}), then the heat pipe could fail to work on-design. Indeed, this undesired

occurrence implies that H_{lv} does not match the heat that is supplied and subtracted from the outside, leading to a overheating of the device. Therefore, a good estimate of the departure of the thermodynamical state of the system from the saturation one is useful to evaluate *a posteriori* one of the possible operating limits, which is a critical supplied power, above which the heat pipe fails and, consequently, to forecast this failure. For this purpose, T_{sat} is determined with the aid of the Clausius-Clapeyron formula (12), and then compared with the output temperature T_{v}. In our case study, the absolute difference $|T_{\text{v}} - T_{\text{sat}}(p)|$ remains less than 1 K almost everywhere in those numerical tests that reproduce a successful experiment. For instance, in the case reported in Fig. 3-a, the relative difference, expressed as a percentage, is very small and presents a peak in the two ends of the pipe ($|T - T_{\text{sat}}|_{\text{max}} \approx 7$ K in the evaporation zone, and $|T - T_{\text{sat}}|_{\text{max}} \approx 3$ K in the condenser). Moreover, at the two ends, $T_{\text{v}} = T_{\text{l}}$, as an evidence of the isothermal phase change.

(a)   (b)
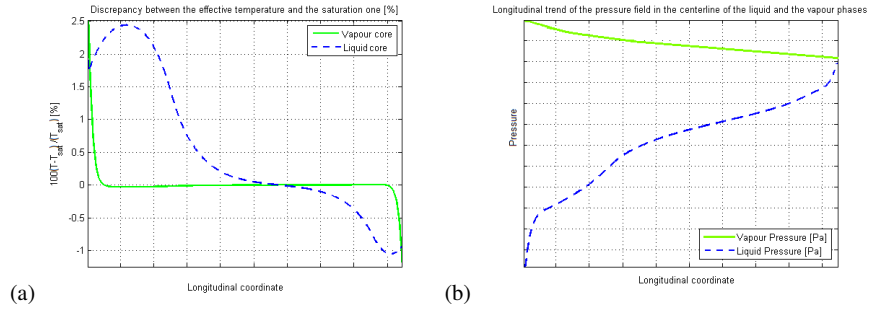
Fig. 3 (a) Relative discrepancy (%) between the computed saturation temperature and T_{v} and T_{l}, respectively. (b) Longitudinal trend of the pressure field in the vapour and in the liquid core.

Another failure of the heat pipe is represented by a loss in capillary pressure of the liquid film. This occurrence can be produced by the high viscosity of the chosen fluid, or a too small capillary pressure, which instead should guarantee the liquid reflux to the evaporator. The velocity field of the liquid phase must be counter-current to the vapour flux in this device, since the former one has to reach the evaporator, whereas the latter one must flow towards the condenser. In Fig. 3-b, the counter-current nature of the velocity in each phase can be deduced from the longitudinal trend of the pressure. In fact, we note that the pressure drop is positive in the vapour and negative in the liquid. Moreover, the pressure jump $|p_{\text{l}} - p_{\text{v}}|$ rising at the evaporator should be as high as possible. This difference is a measure of the capillary drag that acts on the liquid, thereby allowing for its reflux. In the model presented in this work, however, the wick structure is absent. Nevertheless, the pressure difference $|p_{\text{l}} - p_{\text{v}}|$ gives an estimation of the capillary pressure that is sufficient to ensure the reflux of the liquid to the evaporator. This capillary action is partially ascribable to the contribution of the Korteweg stress to the overall stress tensor defined in (2). From the analysis of Figs. 3-a and 3-b, we can conclude that the considered experimental protocol is on-design.

3 Conclusions

The purpose of this work is to support a conscious industrial design of the optimal heat pipe by providing a mathematical model conceived to be rigorous and efficient, but also manageable and implementable on in-house machines.

A two-phase computational fluid dynamic model for estimating the liquid and vapour thermodynamic state inside a heat pipe is developed. For this purpose, the dissipative aspects of the studied problem have been taken into account, and the model has been elaborated in such a way that the Helmholtz free energy density of the two-fluid system depends both on the phase field and on the first gradient of this order parameter, as is the case in the Cahn-Hilliard theory. As a consequence, the Cahn-Hilliard model for phase transitions is generalised to the non-isothermal case. As obtained from the comparison of the numerical outcomes with the experimental data, provided by Argotec s.r.l., the developed numerical model describes effectively some features of the complicated behaviour of a heat pipe.

After validating the model, particular attention is paid to checking the temperature and pressure fields of the liquid and the vapour phases. All the obtained results can be also used for evaluating a posteriori the operating limits of the heat pipe. Indeed, it seems important to comprehend with an adequate amount of confidence in which way off-design conditions may arise. A useful application of the present model could be put into practice, to refine the design and the industrial production of this particular heat exchanger.

Further characterisations and particularisations of the present mathematical model are the object of current investigations, which aims at suiting the present model to the demands of the company, which busily cooperates in the model development by providing new ideas, new test cases, and new related experimental data.

References

1. Anderson, D.M. & McFadden, G.B.: Diffuse-Interface methods in Fluid Mechanics. In: Annu. Rev. Fluid Mech. **30**, pp.139–165 (1998).
2. Chi, S.W. (1976). *Heat pipe theory and practice*. Hemisphere Publishing Corporation.
3. Hall, M.L., Doster, J.M.: A sensitivity study of the effects of evaporation/condensation accommodation coefficients on transient heat pipe modeling.In: Int J. Heat and Mass Transfer, **33**(3), pp. 465-481 (1990).
4. Jamet, D.: Diffuse interface models in fluid mechanics. In: http://pmc.polytechnique.fr/mp/GDR/docu/Jamet.pdf.
5. Kim, J.: A continuous surface tension force formulation for diffuse-interface models. In: Journal of Computational Physics, **204**, pp.784–804 (2005).
6. Lips, S., Bonjour, J. & Lefèvre, F.: Investigation of evaporation and condensation process specific to grooved flat heat pipes. In: Frontiers in Heat Pipes (FHP), **1**, 023001, (2010).
7. Lowengrub, J. & Truskinovsky, L.: Quasi-Incompressible Cahn-Hilliard fluids and topological transitions. In: Proc. R. Soc. Lond. **454**, pp.2617–2654 (1998).
8. Yue, P., Feng, J.J., C. Liu, C. & Shen, J.: A diffuse-interface method for simulating two-phase flows of complex fluids. In: J. Fluid Mech., **515**, pp. 293317 (2004).